Comparison of S-wave velocity structure beneath the Kaapvaal Craton from surface-wave inversion with predictions from mantle xenoliths

S51C-0058

Angela Marie Larson* and J. Arthur Snoke
Virginia Tech

David E. James
Carnegie Institution/DTM

Jane Gore
University of Zimbabwe

Teresia Nguuri
CTBTO, Vienna International Centre

Background: Southern African Seismic Experiment

Between April 1997 and July 1999, 55 broadband seismographs (REFTEK/STS2) were deployed in southern Africa (see figure 1) as part of a four-year international, multi-institutional, interdisciplinary project to determine the geological processes that led to the formation and stabilization of ancient continental cratons. Approximately 100 km station spacing makes it possible to resolve variations in crustal and upper mantle structure across the major tectonic boundaries of southern Africa from receiver-function and surface-wave inversions.

This research focuses on the Archean Kaapvaal craton, a stable remnant of the Earth's early continental lithosphere, and the Bushveld complex, believed to be the world's largest layered intrusion. Based on body wave tomography (figure 2), the effects of the Bushveld appear to have extended well beyond the outcrop area of the intrusion itself.

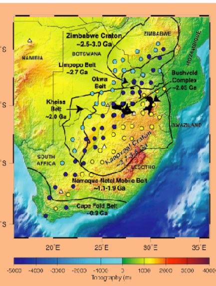

Figure 1: Map showing the principal geologic provinces in southern Africa. Locations of the seismic stations are shown as circles: the dark blue circles represent seismographs deployed for the full two years, while stations that were redeployed are shown first as light blue circles and then as yellow circles. The white triangles are the locations of the GSN stations. The Bushveld Complex outcrop area is marked in black.

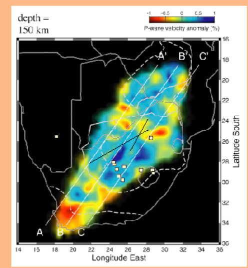

Tomography results

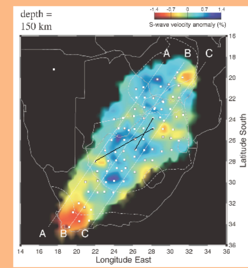

Figure 2: Map view at 150 km depth of P-wave (left) and S-wave (right) velocity perturbations from the inversion of delay times corrected for elevation and crustal thickness. Vertical sections (not shown) indicate that these velocity perturbations do not change significantly with depth between 70 km (the shallowest depth for which the tomography has any resolution) and 200 km depth (the maximum depth for which the surface-wave inversions have any resolution). White squares in the P-wave figure are the xenolith localities. White dots in the S-wave figure represent broadband stations. Black lines show the two paths along which interstation Rayleigh phase velocities were determined for this study. Note that the P-wave tomography shows a significantly decreased velocity in the mantle beneath the Bushveld, but the S-wave tomography shows a more subdued contrast in velocity.

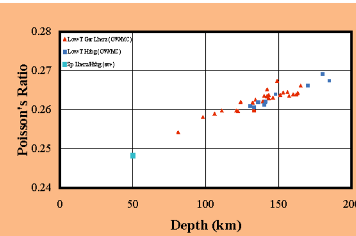

Velocities computed from xenoliths

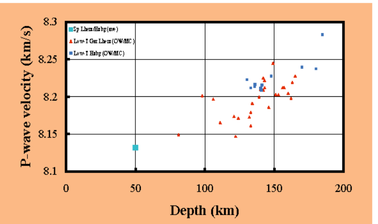

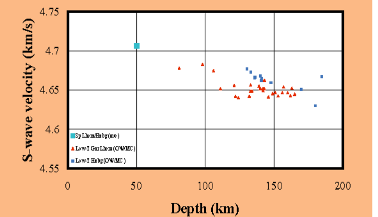

Figure 3: James et al. (2003) computed seismic velocities and rock densities from geothermobarometrically calibrated xenoliths from the Archean Kaapvaal craton. Note the comparatively low Poisson ratio (0.25) in the uppermost mantle as well as the slight decrease of S-wave velocity and increase of P-wave velocity with depth. Linear fits to the velocities, along with densities (not shown), are used to construct the starting model for the upper-mantle velocity structure in the surface-wave inversions. The assumed crustal velocity model of Durheim and Green (1992) was used along with a Moho depth at 38 km, based on the average value from the receiver-function results for the Kaapvaal craton (Nguuri et al., 2001).

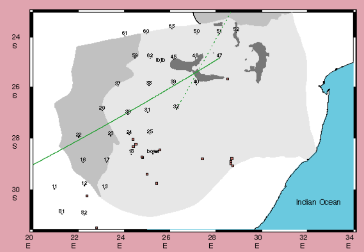

Data preparation: interstation paths

Figure 4: Two events were selected for which the great-circle paths were close to the strike of the network and that have arrivals that show little evidence of multi-pathing: 97130 (Iran, Ms=7.3, 7600 km, BAZ=31deg) and 97288 (Andes, Ms=6.8, 9000 km, BAZ=240deg). Presented here are the results based on four collinear paths from 97288 (solid green line) that include interstation paths ranging from pure craton (SA22-SA39) to pure Bushveld (SA39-SA47) as well as one path (dotted green line) that exhibits very high coherence (SA51-SA32) for event 97130. A short section of some of these paths includes the Kheiss Belt, where the younger Proterozoic has been thrust atop the Archean craton. While the Moho is likely to be complex as a result of the tectonic interaction, the deep crust and (presumably) mantle are Archean in age, hence a cratonic mantle for the Kheiss Belt is assumed. Network stations that recorded these two events are indicated by numbered dots. Filled red squares indicate xenolith localities studied by James et al.

Determination of interstation phase velocities

Interstation fundamental-model Rayleigh phase velocities were calculated for wach station pair using a technique based on Hermann's XSPCRS: the near-station waveform is time shifted to the far-station epicentral distance using a first-order set of phase velocities over the appropriate period range and then fine-tuning with a frequency-domain deconvolution. Estimated errors are based on coherence.

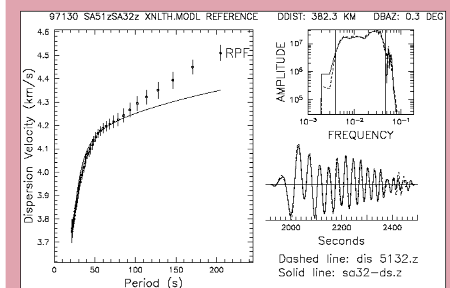

Figure 5: The left-hand panel is the interstation phase velocity vs. period plot for the path between SA51 and SA32 for event 97130. The solid line is the predicted phase velocity curve based on model XNLTH (figure 9). The dotted lines in the plots to the right are for spectral amplitudes and the time series from SA51 (near station) projected to the SA32 (far station) epicentral distance using the phase velocities in the left-hand panel. The solid lines are for the (unaltered) SA32 waveform. The phase-velocity error estimates are based on the coherence between the two time series and show that the phase velocities for this station pair are well constrained up to periods of about 200 seconds.

Craton-Bushveld comparisions

Figure 6: Panels below show four interstation velocity curves along the collinear path from event 97288. SA39-SA47 is only 233 km in length, so it is not as well constrained at periods above 80s. The upper plot demonstrates that all except SA39-SA47 agree at periods longer than 80s indicating that the percentage of the path in the Bushveld does not have a first-order effect on phase velocities at longer periods. The more restricted period range in the lower plot shows that phase velocities in the period range 30-50s decrease as the percentage of the path in the Bushveld increases.

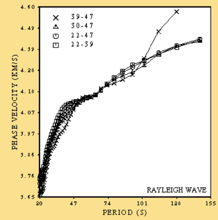

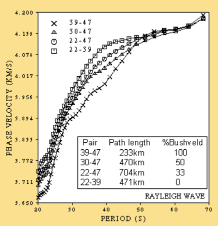

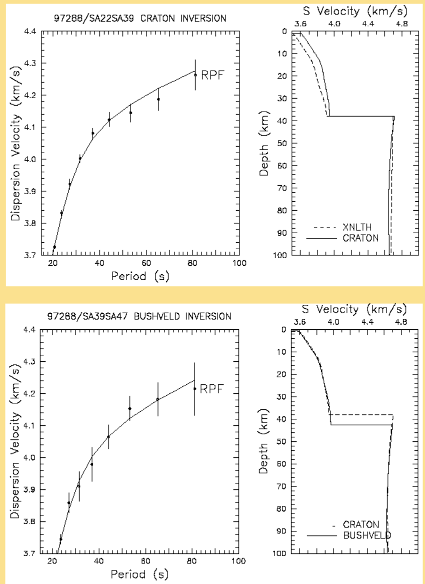

Figure 7: The plots above show that small perturbations in Moho depth can result in acceptable fits for the phase velocities in the period range 30-50s for both the pure craton path (SA22-SA39) and the pure Bushveld path (SA39-SA47). The starting model for the predominantly craton path (upper panel) is XNLTH; for the predominantly Bushveld path (lower panel) it is the same model except the Moho has been shifted from 38 km to 43 km depth. The Bushveld velocities can be fit without shifting the Moho, but only if the velocities are lower both above and below the Moho. As the receiver functions indicate a deeper Moho in the Bushveld and the Bushveld lower crust is thought to be more mafic and hence of a higher velocity, the model shown is the preferred choice. Poisson ratio and density were held constant during inversion. Solid lines are the output Vs models from the inversion, dashed lines are reference models.

Comparing model XNLTH with a surface-wave craton model

To compare the surface-wave model with the model predicted by the xenolith data, well-constrained velocities down to about 180 km depth are needed. Because the coherency for periods above 80s for purely cratonic paths such as SA22-SA39 is poor, one cannot confidently compare phase velocity data directly with phase velocities predicted by XNLTH . Figure 4 shows that the dispersion curve for SA51-SA32 from event 97130 is well constrained to about 200s period and is significantly different from the curve predicted by XNLTH. This station pair is not purely cratonic as it contains a short section through the Bushveld.

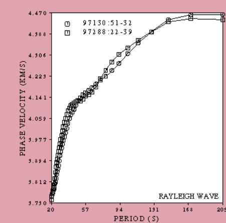

Figure 8: Above are the dispersion curves for SA51-SA32 from event 97130 and the purely cratonic path, SA22-SA39 from event 97288. The phase velocities for these two paths are sufficiently similar enough that one can use the surface-wave inversion for 97130/SA51-SA32 as the starting model to invert 97288/SA22-SA39 for the craton structure. It is relevant here that S-wave tomography indicates relatively small differences between Bushveld and craton at depth (figure 2).

* Contact Information:
Angela Marie Larson
alarson@vt.edu
4044 Derring Hall (0420)
Blacksburg, VA 24061 USA

Velocity models for the Kaapvaal

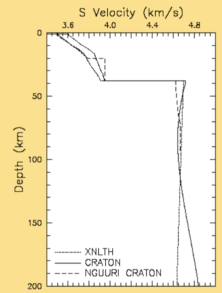

Figure 9: The NGUURI CRATON model is based on 16 paths from three events in the Kaapvaal, but have a maximum period of 102s. Hence the dispersion does not constrain the model at depths greater than about 100 km. Model CRATON (this study) is similar to both NGUURI and XNLTH down to about 100 km depth, but has higher velocities at greater depths.

Reconciling the Xenolith model & surface-wave results

As one can see from figure 9, at depths greater than 100 km, the surface-wave velocity-depth models that are based on observed phase velocities are higher than those predicted from velocities computed from xenolith. While the evidence remains controversial, there is some indication that the deeper xenoliths may record anomalously high temeratures, a result of a thermal perturbation that affected the whole of the southern Kappvaal in Cretaceous time. Thermal diffusion may well have acted to dissipate that perturbation so that present-day geotherm could be lower, meaning that the seismic velocities at depths greater than about 100 km may be higher than indicated from the xenolith studies.